

This article may be downloaded for personal use only. Any other use requires prior permission of the author and APS Publishing.

The following article appeared in *Phys. Rev. Lett.* 110, 088702 (2013) and may be found at <https://doi.org/10.1103/PhysRevLett.110.088702>



## Statistical Similarity between the Compression of a Porous Material and Earthquakes

Jordi Baró,<sup>1,\*</sup> Álvaro Corral,<sup>2</sup> Xavier Illa,<sup>1</sup> Antoni Planes,<sup>1</sup> Ekhard K. H. Salje,<sup>3</sup> Wilfried Schranz,<sup>4</sup>  
 Daniel E. Soto-Parra,<sup>5</sup> and Eduard Vives<sup>1</sup>

<sup>1</sup>*Departament d'Estructura i Constituents de la Matèria, Facultat de Física, Universitat de Barcelona, Martí i Franquès 1, E-08028 Barcelona, Catalonia, Spain*

<sup>2</sup>*Centre de Recerca Matemàtica, Edifici C, Campus Bellaterra, E-08193 Bellaterra, Catalonia, Spain*

<sup>3</sup>*Department of Earth Sciences, University of Cambridge, Downing Street, Cambridge CB2 3EQ, United Kingdom*

<sup>4</sup>*Faculty of Physics, University of Vienna, Boltzmanngasse 5, Vienna A-1090, Austria*

<sup>5</sup>*División de Materiales Avanzados, IPICYT, Camino a la Presa San José 2055, San Luis Potosí, México*

(Received 31 October 2012; published 19 February 2013)

It has long been stated that there are profound analogies between fracture experiments and earthquakes; however, few works attempt a complete characterization of the parallels between these so separate phenomena. We study the acoustic emission events produced during the compression of Vycor (SiO<sub>2</sub>). The Gutenberg-Richter law, the modified Omori's law, and the law of aftershock productivity hold for a minimum of 5 decades, are independent of the compression rate, and keep stationary for all the duration of the experiments. The waiting-time distribution fulfills a unified scaling law with a power-law exponent close to 2.45 for long times, which is explained in terms of the temporal variations of the activity rate.

DOI: [10.1103/PhysRevLett.110.088702](https://doi.org/10.1103/PhysRevLett.110.088702)

PACS numbers: 89.75.Da, 05.65.+b, 62.20.mm, 91.30.Dk

The mechanical failure of materials is a complex phenomenon underlying many accidents and natural disasters ranging from the fracture of small devices under fatigue to earthquakes. Despite the vast separation of spatial, temporal, energy, and strain-rate scales [1,2], and the differences in geometry, boundary conditions, loading, structure of the medium, and interactions, it has been proposed that laboratory experiments on brittle fracture in heterogeneous materials can be a model for earthquake occurrence [3–5]. As the main stresses on Earth's crust are compressive [2], experiments of materials loaded under compression seem the most suitable for drawing analogies with seismicity. But because of the fact that compression stabilizes crack propagation, traditional assumptions applied to samples loaded under tension are not valid in compression, making the compression problem much more challenging conceptually [6].

Some fundamental findings of statistical seismology have also been reported in compressive-failure experiments. First, the Gutenberg-Richter law [7] states that the number of earthquakes as a function of their radiated energy  $E$  decreases as a power law, i.e.,  $p(E)dE \propto E^{-\epsilon}dE$  (with  $\epsilon = 1 + 2b/3$  and  $b$  close to 1). Numerous experiments on compressive failure report power-law distributions in some measure of the size of the events [2,3,8,9]; however, there is considerable scatter in the power-law exponents, which in addition can either decrease with the evolution of the damage [8] or show not so simple variations [2]. In general, external variables have a strong influence on the experiment, mainly on applied stress [2]. Nevertheless, it is possible that some of the early results are artifacts due to low counts and poor statistical analysis.

The existence of power-law distributions and therefore of scale invariance has led some authors to relate fracture with a second-order phase transition [5,6,8], although others point toward a first-order transition [8,10], a debate that replicates in earthquakes [1,10–12]. In any case, the broad range of responses triggered by the usual slow perturbation is the signature of crackling noise [13] (a characterization that does not depend on the underlying mechanisms generating the output of the system).

The (modified) Omori's law [14] accounts for the fact that the number of earthquakes per unit time decreases as a power law since the sudden rise of activity provoked by a “mainshock,” with an exponent  $p$  around 1. The counterparts of this law in fracture have some problems of interpretation (whole rupture of the sample is the mainshock [4] versus similarity should hold also for microfracturing bursts [15]). Further, sometimes it is not possible to distinguish the decay from an exponential form [3,15], or the resulting  $p$  is far from 1, although it has been claimed that the  $p$  exponent decreases as the experiment progresses [15].

The time between consecutive events, or waiting times, have also been measured in experiments under compression [3,8]. The Omori's law implies that the probability density of these times should also follow a power-law decay with an exponent close to 1 [16]. However, the reciprocal is not true, since power-law waiting times do not necessarily imply an underlying Omori's law and therefore are not a proof of the fulfillment of this law.

A coherent picture of waiting times in statistical seismology did not start to consolidate until Bak *et al.* proposed their unified scaling law [17], measuring waiting times above a minimum energy in different regions

together. All the dependence on the size of the regions and on the minimum energy turned out to be governed solely by a unique parameter: the mean seismic activity rate  $\langle r \rangle$ , in such a way that the waiting-time probability density fulfills a scaling law,  $D(\delta) = \langle r \rangle \Phi(\langle r \rangle \delta)$ , with  $\delta$  the waiting time and the scaling function  $\Phi$  showing a power-law decay with exponent  $1 - \nu$  around 1 for small arguments and another power law with exponent  $2 + \xi$  above 2 for large arguments [18]. Although the first exponent is a consequence of the Omori's law, the second one is genuinely new, related to the distribution of background seismic rates [16].

Compression experiments have shown good agreement with a restricted version of this law [9], which considers the special case of a single spatial region and a regime of stationary seismicity (eliminating time periods with Omori-like decay [19]). In this case the scaling function turns out to be well approximated by a flatter power-law decay (with  $1 - \nu$  around 0.3), followed by an exponential decay [19,20].

Finally, another fundamental statistical law of seismic occurrence is the productivity law [21], which establishes that the rate of earthquakes (i.e., aftershocks) triggered by a mainshock of energy  $E$  is proportional to  $E^{2\alpha/3}$ , with  $\alpha \simeq 0.8$ . As far as we know this law has not been reproduced in brittle fracture experiments but in plastic deformation [22].

Therefore, there is no single compressive-failure experiment that reproduces simultaneously the above mentioned fundamental laws of statistical seismicity (Gutenberg-Richter, Omori, productivity, and the unified waiting-time scaling law). The situation for tensile failure and other types of tests is analogous [5,8,23,24], although the results of Ref. [25] are particularly notable, including spatial measurements.

In this Letter we report on the failure under compression of a highly porous material, showing that the four main laws of statistical seismicity hold, with unprecedented statistics, and with robust exponents across different experiments. In contrast to the other laws, the unified scaling law, which yields the best quantitative agreement with earthquakes, is not stationary but arises from the temporal variations of the activity rate.

We perform uniaxial compression experiments of Vycor, a mesoporous silica ceramics (40% porosity), loaded at a constant compression rate  $R$  for three different experiments at  $R = 0.2, 1.6,$  and  $12.2$  kPa/s (considering that the section of the sample keeps constant). Compression is applied without lateral confinement until the shrinkage of the samples is above 20%, leading to multifragmentation. Simultaneous recording of acoustic emission (AE) is performed by using a detector coupled to the upper compression plate. The signal is preamplified (60 dB), band filtered (between 20 kHz and 2 MHz) and analyzed by means of a PCI-2 acquisition system from Euro Physical Acoustics (Mistras Group) working at  $10^6$  samples per second. An

AE avalanche event starts at the time  $t_i$  when the preamplified signal  $V(t)$  crosses a fixed threshold of 26 dB, and finishes when the signal remains below threshold for more than 200  $\mu$ s. The energy  $E_i$  associated with each event  $i$  is computed as the integral of  $V^2(t)$  for the duration of the event divided by a reference resistance. More details of the experiment can be found in Ref. [26].

Figure 1(a) shows an example of the raw results for the experiment at  $R = 1.6$  kPa/s. The jerky evolution of the specimen's height is apparent, as well as the broad range of values of the event energy detected at the transducer. Another view of this intermittent dynamics is provided in Fig. 1(b) by the AE activity rate  $r(t)$  (counting events every 60 s) and the cumulative number of events,  $N(t) = \int_0^t r(t) dt$ . Despite an apparent correlation between the most energetic events and large changes in height, one also observes regions with high acoustic activity not associated with noticeable sample shrinkage.

Figure 2 shows the histograms that estimate the probability densities of the energies [26,27], considering time windows of  $3 \times 10^3$  s. All the distributions show a power-law behavior  $p(E) \propto E^{-\epsilon}$ , with an exponent in the range  $\epsilon = 1.40 \pm 0.05$ , stable for the whole experiment; this is the signature of a remarkable stationarity in the energy dissipation, which appears as independent of applied stress, in contrast to previous works [8] (therefore, the apparent nonstationarity of  $E$  in Fig. 1 is due to a much larger number of events in the central part). The value of the exponent, obtained by maximum likelihood (ML) estimation [27], holds for about 7 decades and is robust against the thresholding of the data (fitting only values of  $E$  larger than  $E_{\min}$ ) and quite independent of  $R$ , as shown in the inset of Fig. 2 [26–28]. Although the resulting exponent turns out to be below the most accepted value for

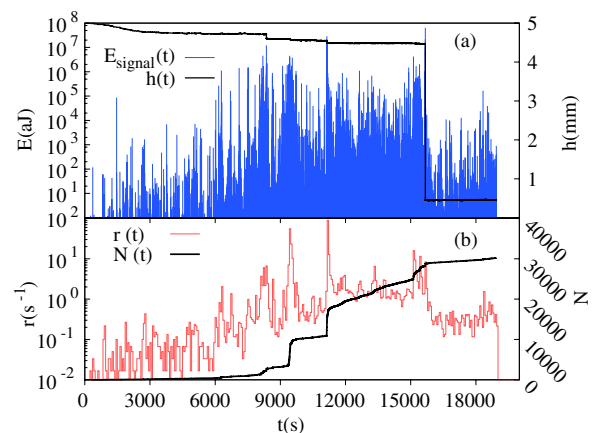


FIG. 1 (color online). (a) Example of the outcome of a compression experiment at  $R = 1.6$  kPa/s, showing the change in the specimen's height  $h$  versus time (proportional to stress) and the energy of the AE avalanches, in logarithmic scale. (b) Time evolution of the AE activity rate and of the total number of events.

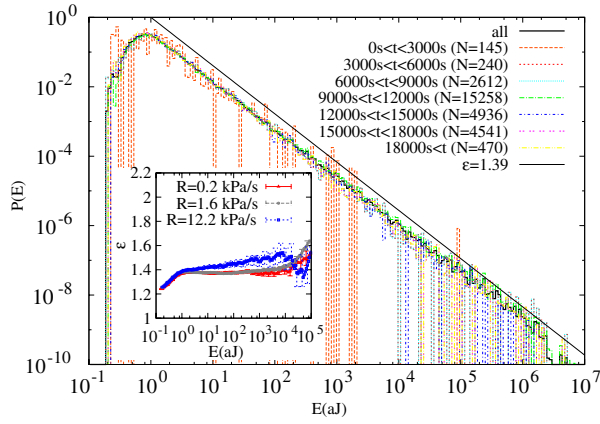


FIG. 2 (color online). Distribution of avalanche energies during the full experiment with  $R = 1.6$  kPa/s and during 7 different subperiods. The line shows the behavior corresponding to  $\epsilon = 1.39$ . The inset shows the ML-fitted exponent  $\epsilon$  as a function of a lower threshold  $E_{\min}$  for the three experiments.

earthquakes,  $\epsilon \approx 1.67$ , Kagan has noticed that this value is inflated due to systematic biases and one could instead expect  $\epsilon$  close to 1.5 (i.e.,  $b \approx 3/4$ ) [29]. Reciprocally, systematic biases of the energy cannot be completely ruled out in AE experiments [5,8].

The next step in our analysis has been the computation of the number of aftershocks (AS) in order to compare it with Omori's law for earthquakes. We have considered as mainshocks (MS) all the events with energies in a certain predefined energy interval. After each MS we study the

sequence of subsequent events until an event with an energy larger than the energy of the MS is found, which finishes the sequence of AS. Then we divide the time line from the MS toward the future in intervals, for which we count the number of AS in each of them. Averages of the different sequences corresponding to all MS in the same energy range are performed, normalizing each interval by the number of sequences that reached such a time distance. The results presented in Figs. 3(a)–3(c) show that the tendency to follow Omori's law is clear, in some cases for up to 6 decades, with an exponent  $p = 0.75 \pm 0.10$ . (compare with Ref. [30]). Foreshocks, obtained in an analogous way, show a similar behavior, with a slightly smaller value of  $p$ .

The previous Omori's plot allows us to also estimate the exponent  $\alpha$  of the productivity law, by rescaling the vertical axis with  $E^{2\alpha/3}$ , finding the optimum  $\alpha$  which leads to the collapse of the data; i.e.,  $r_{AS}/E^{2\alpha/3}$  should be only a function of the time since the mainshock. The results in Fig. 3(d) show that  $\alpha = 0.5 \pm 0.1$ . This is again somewhat smaller than the counterpart for earthquakes, but the drift is compatible with the one found for the energy distribution, in other words, the ratio of exponents  $(\epsilon - 1)/\alpha$  is the same. Remarkably, a collapse can be obtained not only for mainshocks of different energies in the same experiment but also across experiments with different  $R$ , rescaling  $r_{AS}$  as  $r_{AS}E^{-2\alpha/3}/\langle r_R \rangle$ , and the time since the MS,  $t - t_{MS}$ , as  $(t - t_{MS})\langle r_R \rangle$ , with  $\langle r_R \rangle$  giving the mean number of events per unit time.

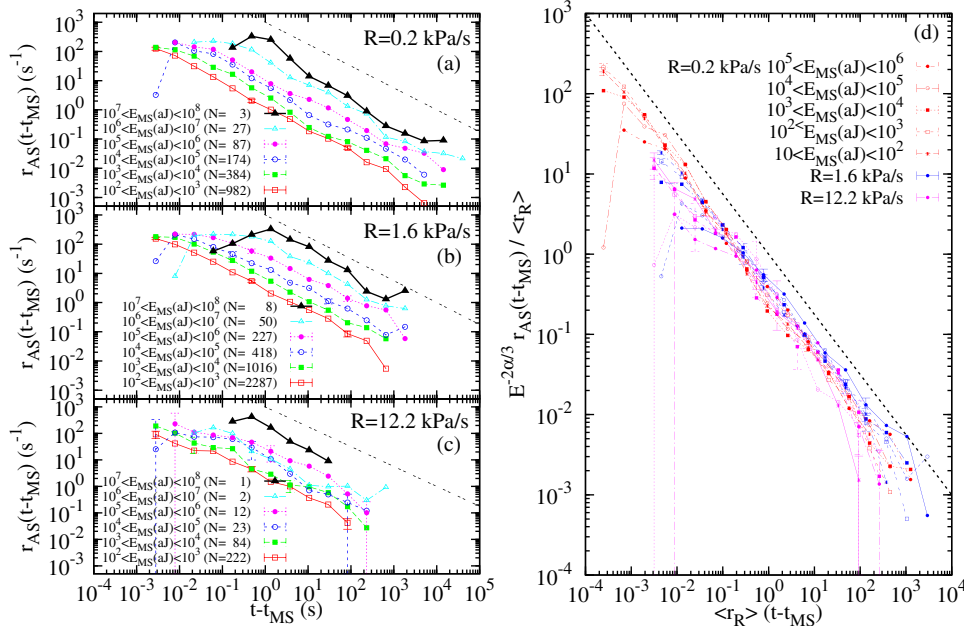


FIG. 3 (color online). (a)–(c) Number of aftershocks per unit time,  $r$ , as a function of the time distance to the main shock for different compression rates in each panel, as indicated by the legend. MS are defined as the events in the energy range indicated by the legend.  $N$  values indicate the number of sequences analyzed for each range. The dashed line indicates the Omori's behavior with slope  $-0.75$ . (d) Rescaled Omori plot showing the fulfillment of the productivity law, with  $\alpha \approx 0.5$ .

These results already suggest that there is a certain similarity in the correlation between avalanches that extends from geophysical scales of the order of hundreds of kilometers to our small samples with cracks much smaller than the mm scale. To deepen into the comparison we have proceeded to the analysis of the interevent or waiting times, defined as  $\delta_j = t_j - t_{j-1}$ , with  $j$  labeling only the events with energy larger than a given  $E_{\min}$ . The estimations of the waiting-time probability densities,  $D(\delta; E_{\min})$ , for different  $E_{\min}$  and different experiments are shown in Fig. 4(a), displaying a power-law decay with exponent  $1 - \nu = 0.93 \pm 0.05$  for most of the time range, as implied by the Omori's law. In order to compare the shape of the distributions we rescale the axes as  $\langle r(E_{\min}) \rangle \delta$  and  $D(\delta; E_{\min}, R) / \langle r(E_{\min}) \rangle$ , with  $\langle r(E_{\min}) \rangle$  giving the mean number of events per unit time with  $E \geq E_{\min}$ . Figure 4(b) shows how the different distributions collapse into a single one, signaling the existence of a scaling law; for a single experiment, as the activity rate verifies the Gutenberg-Richter law, the collapse “unifies” this law with the temporal properties [17]. For different experiments the collapse implies the similarity versus the compression rate  $R$ . Moreover, the plot also shows that a second power law emerges for the rightmost tail of the distributions, with an exponent  $2 + \xi = 2.45 \pm 0.08$  [31].

To make clear the correspondence with earthquakes, Fig. 4(b) also includes seismic data for different spatial windows in Southern California [17,18]. Although the previously reported value of  $\xi$  for earthquakes [18] is a bit smaller than for the experiment, the similarity is remarkable, taking into account that the earthquake measurements are taken over different spatial windows, whereas for the AE data we do not have access to such degrees of freedom.

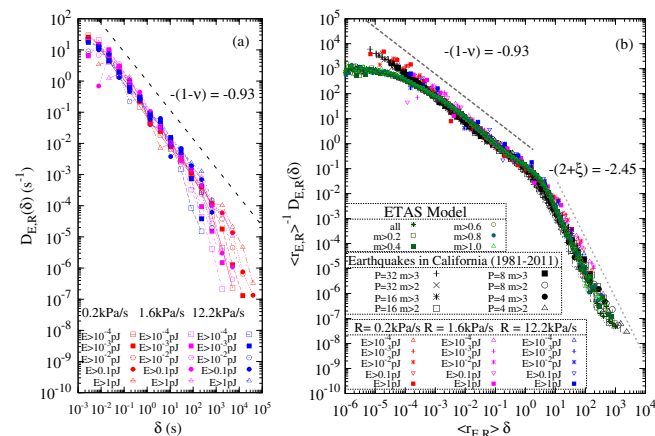


FIG. 4 (color online). (a) Distribution of waiting times for different values of  $E_{\min}$  and the compression rate  $R$ . (b) The same data under rescaling, also including the results of the ETAS model and earthquakes from Southern California divided into  $P \times P$  regions [17,18] for the period January 1984–June 2011.

How then can we get essentially the same behavior in such different situations? The answer lies in the variations of the activity rate. Let us consider a single Omori sequence, for which the waiting-time density depends on the background activity rate  $\mu$  through a scaling form [16],

$$D(\delta|\mu) = \frac{\mu}{(\mu\delta)^{1-\nu}} f(\mu\delta), \quad (1)$$

where  $\nu$  is close to 0 and  $f$  can be a decreasing exponential, or another function showing the same behavior at 0 and  $\infty$ . If the background rate is not fixed but evolves during the experiment, the resulting density will be

$$D(\delta) \propto \int_{\mu_{\min}}^{\mu_{\max}} d\mu \rho(\mu) \mu D(\delta|\mu), \quad (2)$$

where  $\rho(\mu)$  is the density of background rates. Substituting the previous equation and considering that  $\mu$  is broadly distributed between  $\mu_{\min}$  and  $\mu_{\max}$  with  $\rho(\mu) \propto 1/\mu^{1-\xi}$  leads to  $D(\delta) \propto 1/\delta^{1-\nu}$  for  $\delta \ll \mu_{\max}^{-1}$  (because the rescaled integral goes to zero as  $\delta^{1+\xi+\nu}$ ) but  $D(\delta) \propto 1/\delta^{2+\xi}$  for  $\delta \gg \mu_{\max}^{-1}$  (because the rescaled integral converges to a constant). This behavior for  $\rho(r)$  can arise from a time evolution of the form  $\mu(t) \propto t^{1/\xi}$ , as  $\rho(\mu) \propto |dt/d\mu(t)|$  [16]. So, when the background rate varies across different scales [as in Fig. 1(b)] and this takes place through a power law, a second power law arises in  $D(\delta)$ . The experimental outcome suggests then  $\xi \simeq 0.5$ . We have simulated the epidemic type aftershock (ETAS) model [32], defined by the fact that each earthquake  $i$ , with a Gutenberg-Richter energy, triggers a sequence with a rate equal to  $KE_i^{2\alpha/3}/(c+t-t_i)^{1+\theta}$ , and the overall rate is the linear superposition of these rates plus a background rate. The “microscopic” exponent  $1 + \theta$  corresponds to an observable  $p = 1 - \theta$  [32]. Using as input the experimental values of  $\epsilon$ ,  $p$ , and  $\alpha$ , together with  $c = 0.001$  s, and  $\mu$  increasing slowly as  $\mu(t) \propto 1 - \cos\omega t$  (essentially a power law with  $\xi = 1/2$ ), we obtain very good concordance with the previous calculations [see Fig. 1(b)] when the branching ratio {given by  $Kb/[\theta c^\theta(b - \alpha)]$ } is very close to criticality, i.e., 0.99. In addition, the measurement of  $r(t)$ , using different time intervals, leads to a distribution with a power-law tail of the form  $1/\sqrt{r}$  for small  $r$  (not shown). This explanation could hold also for Ref. [33].

In summary, we have presented experimental results on the compression of a highly porous material, obtaining good fulfillment of some fundamental laws of statistical seismology. Laws involving the measurement of energy and the Omori's law show some bias in the exponent with respect to the earthquake case, whereas for the unified scaling law the quantitative agreement is much better. However, the explanation of the emergence of a power-law tail in the unified scaling law (exponent  $2 + \xi$ ) is different from the one given in previous studies of earthquakes [16,18]. In our compression experiment the spatial variation of the background activity ( $\mu$ ) is not the cause of

the power law, but instead its temporal variation  $\mu(t)$  is the cause. These broad variations of the activity rate were filtered in previous compression experiments, thus rendering a different observed behavior. As our experiment does not allow the measurement of the location of the events, it has not been possible to test laws regarding spatial properties, which also constitute an important body of knowledge for the characterization of seismicity [25]. This should be undertaken in the future with the simultaneous use of many AE sensors, which would allow a more accurate comparison between failure under compression and earthquakes.

We acknowledge financial support from the Spanish Ministry of Science (MAT2010-15114 and FIS2009-09508), the Leverhulme Foundation (RG66640) and EPSRC (RG66344), and the Austrian Science Fund (FWF) P23982-N20. X. I. and E. V. acknowledge the hospitality of the Aspen Center for Physics which is supported by the NSF, Grant No. PHY-1066293.

---

\*jordibaro@ecm.ub.edu

- [1] Y. Ben-Zion, *Rev. Geophys.* **46**, RG4006 (2008).
- [2] I. Main, *Rev. Geophys.* **34**, 433 (1996).
- [3] K. Mogi, *Bulletin of the Earthquake Research Institute, University of Tokyo* **40**, 125 (1962).
- [4] C. H. Scholz, *Bull. Seismol. Soc. Am.* **58**, 1117 (1968).
- [5] D. Bonamy, *J. Phys. D* **42**, 214014 (2009).
- [6] L. Girard, J. Weiss, and D. Amitrano, *Phys. Rev. Lett.* **108**, 225502 (2012).
- [7] T. Utsu, *Pure Appl. Geophys.* **155**, 509 (1999).
- [8] M. J. Alava, P. K. V. V. Nukala, and S. Zapperi, *Adv. Phys.* **55**, 349 (2006).
- [9] J. Davidsen, S. Stanchits, and G. Dresen, *Phys. Rev. Lett.* **98**, 125502 (2007).
- [10] J. B. Rundle, D. L. Turcotte, R. Shcherbakov, W. Klein, and C. Sammis, *Rev. Geophys.* **41**, 1019 (2003).
- [11] P. Bak, *How Nature Works: The Science of Self-Organized Criticality* (Copernicus, New York, 1996).
- [12] D. Sornette, *Critical Phenomena in Natural Sciences* (Springer, Berlin, 2004), 2nd ed.
- [13] J. P. Sethna, K. A. Dahmen, and C. R. Myers, *Nature (London)* **410**, 242 (2001).
- [14] T. Utsu, Y. Ogata, and R. S. Matsu'ura, *J. Phys. Earth* **43**, 1 (1995).
- [15] T. Hirata, *J. Geophys. Res.* **92**, 6215 (1987).
- [16] A. Corral and K. Christensen, *Phys. Rev. Lett.* **96**, 109801 (2006).
- [17] P. Bak, K. Christensen, L. Danon, and T. Scanlon, *Phys. Rev. Lett.* **88**, 178501 (2002).
- [18] A. Corral, *Physica (Amsterdam)* **340A**, 590 (2004).
- [19] A. Corral, *Phys. Rev. Lett.* **92**, 108501 (2004).
- [20] A. Saichev and D. Sornette, *Phys. Rev. Lett.* **97**, 078501 (2006).
- [21] A. Helmstetter, *Phys. Rev. Lett.* **91**, 058501 (2003).
- [22] J. Weiss and M. C. Miguel, *Mater. Sci. Eng. A* **387-389**, 292 (2004).
- [23] K. Mogi, *Tectonophysics* **5**, 35 (1967).
- [24] J. Åström *et al.*, *Phys. Lett. A* **356**, 262 (2006).
- [25] M. Grob, J. Schmittbuhl, R. Toussaint, L. Rivera, S. Santucci, and K. J. Måløy, *Pure Appl. Geophys.* **166**, 777 (2009).
- [26] E. K. H. Salje, D. E. Soto-Parra, A. Planes, E. Vives, M. Reinecker, and W. Schranz, *Philos. Mag. Lett.* **91**, 554 (2011).
- [27] J. Baró and E. Vives, *Phys. Rev. E* **85**, 066121 (2012).
- [28] The small deviation corresponding to the largest compression rate  $R = 12.2$  kPa/s can be due to some nontrivial effects of overlapping and/or distortion of the avalanches.
- [29] Y. Y. Kagan, *Tectonophysics* **490**, 103 (2010).
- [30] D. Sornette and G. Ouillon, *Phys. Rev. Lett.* **94**, 038501 (2005).
- [31] On the other hand, if we restrict to stationary conditions (constant activity rate) the behavior is then similar to that of Refs. [9,19,24].
- [32] A. Helmstetter and D. Sornette, *J. Geophys. Res.* **107**, 2237 (2002).
- [33] S. Santucci, L. Vanel, and S. Ciliberto, *Eur. Phys. J. Special Topics* **146**, 341 (2007).